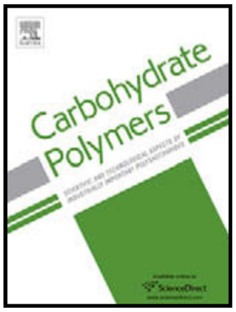

Title: Properties of Rosin-Based Waterborne
Polyurethanes/Cellulose Nanocrystals Composites

Author: He Liu Shuqin Cui Shibin Shang Dan Wang Jie Song

PII: S0144-8617(13)00363-9
DOI: http://dx.doi.org/doi:10.1016/j.carbpol.2013.04.010
Reference: CARP 7626

To appear in:

Received date: 25-2-2013
Revised date: 18-3-2013
Accepted date: 9-4-2013

Please cite this article as: Liu, H., Cui, S., Shang, S., Wang, D., & Song, J., Properties of Rosin-Based Waterborne Polyurethanes/Cellulose Nanocrystals Composites, *Carbohydrate Polymers* (2013), http://dx.doi.org/10.1016/j.carbpol.2013.04.010

Properties of Rosin-Based Waterborne Polyurethanes/Cellulose Nanocrystals Composites

He Liu, [a] Shuqin Cui, [a] Shibin Shang,*[a,b] Dan Wang [a,b], and Jie Song [c]

[a] Institute of Chemical Industry of Forestry Products, Chinese Academy of Forestry; Key Lab. of Biomass Energy and Material, Jiangsu Province; National Engineering Lab. for Biomass Chemical Utilization; Key and Lab. on Forest Chemical Engineering, SFA, Nanjing 210042, China.

[b] Institute of New Technology of Forestry, Chinese Academy of Forestry, Beijing 100091, China.

[c] Department of Chemistry and Biochemistry, University of Michigan-Flint, Flint MI 48502, United States.

Corresponding author footnote: 16 Suojin Wucun, Nanjing 210042, China. Tel: +86 25 85482499; Fax: +86 25 85482499; E-mail:shangsb@hotmail.com

Highlights:

►Novel rosin-based waterborne polyurethanes and cellulose nanocrystals composites were prepared.

►Cellulose nanocrystals were compatible with rosin-based waterborne polyurethanes.

►Thermal stability of rosin-based waterborne polyurethanes was improved by cellulose nanocrystals.

►Tensile strength of waterborne polyurethanes was improved significantly by rosin and cellulose nanocrystals.

Abstract

Polymers from renewable biomass are viable supplements for synthetic polymers. In this study, cellulose nanocrystals (CNs) were used as nanofillers to improve properties of rosin-based waterborne polyurethanes (RWPU). The morphology, structure, thermal, and mechanical properties of the RWPU/CNs nanocomposites were investigated. It demonstrated that CNs were compatible with RWPU and dispersed homogeneously in the polymer matrix. CNs as nanofillers improved tensile strength of RWPU significantly. Tensile strength of RWPU/CNs composite films increased from 28.2 to 52.3 MPa with increasing CNs amount from 0 to 20 wt%. Moreover, the thermal stability of RWPU was also improved by CNs and the glass transition temperature of RWPU/CNs decreased comparing with RWPU. This work provided a novel pathway for preparation of biomass-based WPU with excellent properties from cellulose and rosin.

Key words: Cellulose Naocrystals, Rosin, Waterborne Polyurethanes, Nanocomposite

1. Introduction

Polyurethanes (PU) are polymeric materials that are widely used in coatings and adhesives industries, and finding their way into other high performance niche applications (Chattopadhyay & Raju, 2007). The use of PU is mainly in solvent borne systems. As more people are becoming more environmentally conscious, research on the development of new coating systems to minimize volatile organic compounds have been motivated (Noble, 1997). Waterborne Polyurethanes (WPU) are fully reacted urethane polymers dispersed in water, which shows many excellent features compared to conventional organic solvent-based polyurethane. However, some defects, such as low mechanical strength and thermal stability, restrict the application of WPU. In the past decades, research on high performance WPU focuses on two aspects, molecular design of WPU and hybridizing with other materials (Ma & Zhang, 2009; Naghash & Abili, 2010; Cao et al., 2008; Lee & Kim, 2012).

The effective ways to improve the properties of WPU are through chemical modification of their structures and hybridizing with nanomaterials (Chattopadhyay & Raju, 2007; Althues et al, 2007). Molecular chemical modification is aimed at two aspects, either changing the hard and soft segments of WPU or introduction of chemical crosslink. In the first aspect, WPU can be described as block copolymer composed of hard and soft segments. The intrinsic incompatibility or thermodynamic immiscibility between hard and soft segments causes phase separation. Degree of the hard and soft phase separation plays a vital role in determining the solid-state properties of WPU. In the second aspect, chemical crosslink produces a three-dimensional network structure of WPU which restricts the movement of soft segments and reduces macromolecular degradation to a negligible amount (Cooper & Tobolsky, 1966; Chang et al., 1998). So an appropriate chemical crosslink is beneficial to improve the mechanic strength and thermal stability of WPU. Furthermore, the hybridization of WPU and fillers not only improves, but also provides WPU with some new properties (Althues et al., 2007). A low volume fraction of fillers, especial nanofillers, can significantly induce change in properties of WPU. Commonly, the fillers can be divided into two descriptions: inorganic materials like clay (Rahman et al., 2008), silica (Lee et al., 2011), grapheme (Wang et al., 2012), and zinc oxide (Ma & Zhang, 2009) etc. in nanosize, and organic polymers like polyacrylate (Song et al., 2004), polyaniline (Chen et al., in press), vinyl acetate-acrylic (Naghash & Abili, 2010), cellulose (Cao et al., 2009; Wang et al., 2010; Gao et al, 2012), starch (Zou et al, 2011; Lee & Kim, 2012) and chitosan (Nikjea & Tehrania, 2010) etc. Some of these polymers exist in natural resources, which show numerous benefits to human beings.

Biomass is an abundant carbon-neutral renewable resource. As a viable supplement to fossil fuel resources, biomass is available for the production of energy and materials. In the past decade, numerous research interests are greatly focusing on the hybrid materials consisted of WPU and natural polymers. Cellulose nanocrystals (CNs), with a high bending strength, a high Young's modulus and low density, employed as nanofillers to reinforce WPU was first discussed by Cao and coworkers (Cao et al., 2007). The WPU/CNs showed a significant increase in tensile strength from 4.27 to 14.86 MPa with increasing filler content from 0 to 30 wt %. Subsequently, Cao et al. adopted another method to synthesize a series of new WPU/CNs composites via in situ polymerization, which induced the grafting part of the pre-synthesized WPU chains on the surface of CNs. Tensile strength of WPU increased from 4.4 to 9.7 MPa in the condition of the CNs content range from 0 to 10 wt% (Cao et al., 2009). In addition, some works about CNs, starch, and chitosan hybridizing with WPU to improve the mechanic strength or thermal stability were carried out (Gao et al, 2012; Lee & Kim, 2012; Nikjea & Tehrania, 2010). These novel materials are eco-friendly and biodegradable, which have a broad potential application in various fields.

Therefore, biomass becomes a competitive supplement to high performance WPU materials.

In our previous work, derivatives of pimaric acid which is the most content of rosin reacted with diols as main chains of WPU (Xu et al, 2011a,b). The hydrophenanthrene moiety, consisting of fused cycloaliphatic and aromatic structures, provides rosin acids with substantial hydrophobicity and rigidity. These properties can potentially provide beneficial applications with improved mechanical properties, thermal stability, and water resistance of rosin-based WPU. We also prepared CNs/Ag nanoparticles (AgNPs) composites as bifunctional nanofillers within WPU (Liu et al, 2012). The CNs/AgNPs not only improve the mechanical strength, but it also provides antimicrobial activity to WPU composites. However, overfilled filling of CNs will reduce the tensile strength of WPU due to the aggregation of nanofillers. It is proved that the extent of the reinforcement depends on such factors such as the dispersion of the nanofillers in the polymer matrix and the interfacial adhesion between nanofillers and polymer matrix (Habibi & Dufresne, 2008; Habibi et al, 2008). Therefore, the compatibility of CNs in rosin-base WPU and properties of rosin-based WPU/CNs composites are our research interests. In our current work, CNs isolated from microcrystalline cellulose (MCC) by sulphuric acid hydrolysis incorporated into rosin-based WPU to be novel composites. Rosin-based WPU (RWPU) was prepared according to our previous work. RWPU/CNs composites were prepared by casting the mixture of CNs aqueous suspensions and emulsion of RWPU with various contents. The morphology and performance of RWPU/CNs composites were investigated and characterized.

2. Experimental

2.1. Materials

Rosin was supplied by Wuzhou Pine Chemicals Ltd (Guangxi, China). Polyether glycol N-210 (average molecular weight 1000 g/mol) was obtained from Sinopharm Chemical Reagent Co. Ltd (Shanghai, China). 2,4-Toluene diisocyanate (TDI) was purchased from Jiangbei Chemical Reagents Factory (Wuhan, China) and redistilled before use. Dimethylol propionic acid and dibutyl tin dilaurate of synthetic grade were purchased from First Chemicals of Tianjin (Tianjin, China). Triethylamine and diethylene glycol (DEG) were from Lingfeng Chemicals of Shanghai (Shanghai, China). The polyol, dimethylol propionic acid and DEG were dehydrated at 100 ^{o}C in vacuum for 24 h before use. Sulfuric acid (H_2SO_4, 98 wt %) and microcrystalline cellulose (MCC) were purchased from Sinopharm Chemical Reagent Co., Ltd. and used without further purification.

2.2. Synthesis of rosin-based waterborne polyurethane

The preparation of rosin-based waterborne polyurethane (RWPU) was described by our previous works (Xu et al, 2011a,b). Fumaropimaric acid (FPA) was first synthesized from rosin. Mixture of rosin and fumaric acid was maintained at 220 ^{o}C for 3 h under a dry nitrogen atmosphere and weight ratio of rosin and fumaric was 5:1 as well. After cooled to room temperature, FPA was obtained. Second, fumaropimaric acid polyester polyol (FAPP) was synthesized from FPA (200.0 g) reacting with DEG (76.2 g) at 220 ^{o}C for 3 h under reduced pressure. The reaction was terminated when the acid value was reduced to less than 10 mg/g. Finally, FAPP and polyether glycol N-210 that total weight was 25.0 g and weight ratio was 3:7 reacted with TDI (13.5 g) and dimethylol propionic acid (2.2 g) at 85 ^{o}C. Then acetone was slowly added to obtain a homogeneous mixture and maintained at 85 ^{o}C for 3 h. The prepolymer was extended by addition of DEG (2.5 g), and allowed to react at 60 ^{o}C for 3 h. The mixture was then neutralised by addition of triethylamine (2.0 g) under stirring at 30 ^{o}C for 30 min. Dispersion was accomplished by slowly adding water (100.8 g) to the neutralized polyurethane solution with vigorous stirring. After removing the acetone (by evaporation at 35 ^{o}C in a rotary evaporator under reduced pressure), RWPU with about 30 wt% solids content was obtained. WPU with about 30 wt% solids content without rosin was also prepared in the same condition.

2.3. Preparation of Cellulose Nanocrystals

Microcrystalline cellulose (6 g) was mixed with sulfuric acid solution (90 mL, 64 wt %) and the mixture was stirred vigorously at 40 °C for 2 h. The suspension was then diluted ten times to stop the reaction. The suspension of pH 2 was obtained by centrifuging and washing the CNs suspension with water repeatedly. Dialysis was performed to remove free acid in the suspension, and the result was monitored by checking the neutrality of the dialysis effluent. CNs powder was finally freezing dried.

2.4. Preparation of RWPU/CNs Nanocomposites Films

The RWPU emulsions (30 wt%) were mixed with aqueous CNs dispersion under sonication for 20 min to obtain suspensions of different compositions. Resulting mixtures were stirred in a rotary evaporator under vacuum for 15 min to remove residual air and avoid the formation of irreversible bubbles during evaporation. Resulting mixtures were subsequently cast in Teflon molds and water was evaporated at room temperature. The dry composites films were roasted at 80 °C for 4 h. A series of nanocomposites films with a thickness of ~0.3 mm were prepared by altering the CNs content over the range of 0, 5, 10, 15, and 20 wt %, and were denoted as RWPU, RWPU/CNs5%, RWPU/CNs10%, RWPU/CNs15%, and RWPU/CNs20%, respectively. Prior to characterization, the resulting films were conditioned at room temperature in a desiccator containing P_2O_5 with 0% relative humidity (RH).

2.5. Characterizations

The morphology of CNs was observed by atomic force microscopy (AFM), using a Multimode SPM (Bruker). AFM samples were typically prepared by dropping the sample suspension on a mica slice, and AFM images of CNs were obtained by tapping mode. Fourier transform infrared (FT-IR) spectra were recorded on an iS10 FT-IR Spectrometer (Nicolet). Scanning electron microscope (SEM) was carried out using a Hitachi S4800, and used to investigate the surface of RWPU-based films. Thermal gravimetric analysis (TGA) was carried out with a TAQ50 system from 100 to 600 ^{o}C at heating rate of 10 ^{o}C/min in air. Differential scanning calorimetry (DSC) of the films was carried out with a DSC200 PC apparatus (Netzsch, Selb, Germany) under a nitrogen atmosphere. Each sample was subjected to heating/cooling cycles between -50 and 100 ^{o}C to obtain reproducible glass transition temperature (Tg) values. The heating rate was 10 ^{o}C/min. The mechanical properties of the RWPU-based films were measured on a universal testing machine (CMT 6503, Shenzhen SANS Test Machine Co. Ltd., China) and an average value of at least five replicates for each sample was taken according to the ASTM D412 standard.

3. Result and Discussion

3.1. Morphologies of CNs and RWPU/CNs

An AFM image of CNs deposited from a dilute suspension is shown in Figure 1, from which it is apparent the suspension contains cellulose fragments. Fragments appear as slender rods of ~10-20 nm in width and ~100-200 nm in length. The surface characterization of RWPU, RWPU/CNs10%, and RWPU/CNs20% films was carried out by SEM. The SEM images in Figure 2a show that no morphology of CNs is observed in the matrix of the neat RWPU film. In contrast, the rod-like morphology of CNs is easily identified in Figure 2b and Figure 2c, which are the surface of RWPU/CNs10% and RWPU/CNs20%, respectively. In our previous work, overfilled filling of CNs will reduce the tensile strength of WPU due to the aggregation of nanofillers (Liu et al, 2012). However, in the current work, surface of the RWPU/CNs films are smooth and have no cracks. Our investigation indicates that no CNs sedimentation or flocculation occurred during the evaporation process. Homogeneous distribution of CNs in the RWPU matrix is observed, which implies there is good compatibility between the fillers and polymeric matrix.

FT-IR spectra of dried RWPU and RWPU/CNs composites are presented in Figure 3. For RWPU film, the stretching vibration of N-H bonds formed by interaction of the -NCO group of TDI with the -OH group on FAPP and polyether glycol N-210 surfaces exhibits a strong absorption peak centered at around 3298 cm^{-1} arising from the hydrogen bonding between NH and carbonyl groups; otherwise the free NH stretching vibration should appear at around 3420 cm^{-1}. With an increase of the content of CNs in the RWPU matrix, a shoulder peak appears at 3335 cm^{-1}. This is attributed to the OH stretching vibration of the CNs.

3.2. Thermal Properties of RWPU/CNs composites

The thermal decomposition behavior of RWPU and RWPU/CNs composites are shown in Figure 4. The RWPU and the CNs composites display a weight loss at temperatures from 100 to 600 ^{o}C. Three obvious stages of decomposition appear at the TGA curves. The first stage is from 100 to 300 ^{o}C and weight loss is from 0 to 20 %. The curves of RWPU and RWPU/CNs composites are similar in this stage, which means that thermal stabilities of RWPU/CNs composites are as same as RWPU. However, in the second stage, the decomposition temperature alters remarkably from 300 to 375 ^{o}C, which implies there is a change in the thermal stability of the composites. The 30 % weight loss temperature of RWPU is 307 ^{o}C, and the temperatures of RWPU/CNs with varying CNs loading level with 10 wt% and 20 wt% are 316 and 334 ^{o}C, respectively. This significant enhancement of thermal resistance caused by CNs can be attributed to the formation of a confined structure in the RWPU/CNs nanocomposites. In the last stage, the residues' mass of RWPU/CNs composites are more than RWPU, which is because of the aromatization of cellulose residue to be graphite.

To further understand the structure and interactions between the two components, DSC studies of the RWPU and RWPU/CNs nanocomposites were conducted. Figure 5 shows the DSC thermograms of RWPU matrix and nanocomposites reinforced with varying amounts of CNs. The values of T_g and the heat capacity change (ΔC_p) are shown in Table 1. According to the results, the T_g decreased as the amount of CNs increased and it varied from 22.54 ^{o}C for neat RWPU to approximately 16.95 ^{o}C for RWPU with a 10% CNs loading. The addition of CNs might interrupt the original interactions between soft segments and hard segments, and improve the microphase separation in RWPU. This effect can indirectly result in a decrease of T_g of soft segments. However, comparing with RWPU/CNs10%, the T_g of RWPU/CNs15% and RWPU/CNs20% increased to 17.07 ^{o}C and 20.80 ^{o}C, respectively. This is the opposite effect of CNs in RWPU matrix. The restricted mobility of RWPU chains neighboring CNs that is due to the co-crystallization event with those grafted on the surface might be the origin of the shift of T_g towards higher temperature. Also, it is hypothesized that this co-crystallization could also enhance the interactions between soft and hard segments; and therefore limits the microphase separation in RWPU, which could also indirectly result in an increase of T_g of the soft segments of RWPU.

3.3. Tensile strength and elongation at break study

The mechanical behaviors of WPU, RWPU, and composites films reinforced with various compositions of CNs were investigated by tensile testing at room temperature. Data showing tensile strength, elongation at break, and Young's modulus are presented in Table 2. Figure 6 shows the evolution of tensile strength and elongation at break, as a function of CNs content for the WPU and RWPU matrix composites films, respectively. Pure WPU showed a low tensile strength of 12.0 MPa, a low Young's modulus of 27.0 MPa, and a high elongation at break of about 971%. CNs content has a significant effect on the mechanical properties of WPU. Tensile strength increased from 12.0 to 29.1 MPa, which represented a ~142% increased, and elongation at break decreased from 971 to 99%, upon increasing CNs content from 0 to 20 wt% of WPU. So the Young's modulus of WPU/CNs composites significantly increased from 27.0 to 457.4 MPa as compared with pure WPU. This indicated that incorporating CNs into the RWPU matrix resulted in strong interactions between the filler and matrix, which restricted the matrix motion. RWPU shows higher tensile strength and lower elongation at break than neat WPU because of the rigid structure of rosin acid. With increasing CNs content from 0 to 20 wt%, tensile strength of RWPU/CNs composite films increased from 28.2 to 52.3 MPa and elongation at break decreased from 267 to 22%. The Young's modulus of RWPU/CNs composites also increased from 316.2 to 1045.4 MPa as compared with RWPU. Elongation at break of RWPU/CNs decreased greatly with increasing CNs content because of restriction between CNs and polymer segments. In addition, tensile strength of RWPU was much higher than most WPU/CNs composites except

WPU/CNs20%. These results indicated that mechanic properties of WPU composites can be improved significantly by incorporating CNs and rosin within the WPU matrix.

4. Conclusion

CNs was prepared and used as nanofiller with varying amount to improve the properties of RWPU. SEM and FT-IR results indicated that CNs was dispersed homogeneously within the RWPU matrix. The filling of CNs into RWPU could lead to a decrease of T_g for RWPU-based composites and improve the thermal decomposition resistance. Tensile strength of RWPU films increased significantly with filling CNs. Elongation at break decreased greatly with increasing CNs content. Comparing with WPU, mechanic properties of RWPU and RWPU/CNs composites were both improved significantly. The results indicated that incorporation with bio-resource, like rosin and CNs, are valuable for the WPU applications.

Acknowledgements

We gratefully acknowledge the financial support from the National Natural Science Foundation of China (Grant No. 31070519).

Reference

Althues, H., Henle, J., & Kaskel, S., (2007). Functional inorganic nanofillers for transparent polymers. *Chemical Society Reviews, 36,* 1454-1465.

Cao, X. D., Chang, P. R., & Huneault, M. A., (2008). Preparation and properties of plasticized starch modified with poly(ε-caprolactone) based waterborne polyurethane. *Carbohydrate Polymers, 71,* 119-125.

Cao, X. D., Dong, H., & Li, C. M., (2007). New nanocomposite materials reinforced with flax cellulose nanocrystals in waterborne polyurethane. *Biomacromolecules, 8,* 899-904.

Cao, X. D., Habibi, Y., & Lucia, L. A., (2009). One-pot polymerization, surface grafting, and processing of waterborne polyurethane-cellulose nanocrystal nanocomposites. *Journal of Materials Chemistry, 19,* 7137-7145.

Chang, S. L., Yu, T. L., Huang, C. C., Chen, W.C., Linliu, K., & Lin, T. L., (1998). Effect of polyester side-chains on the phase segregation of polyurethanes using small-angle X-ray scattering. *Polymer, 39,* 3479-3489.

Chattopadhyay, D. K., & Raju, K. V. S. N., (2007). Structural engineering of polyurethane coatings for high performance applications. *Progress in Polymer Science, 32,* 352-418.

Chen, C. H., Kan, Y. T., Mao, C. F., Liao, W. T., & Hsieh, C. D., Fabrication and characterization of water-based polyurethane/polyaniline conducting blend films. *Surface & Coatings Technology, doi:10.1016/j.surfcoat.2012.03.056.*

Cooper, S. L., & Tobolsky, A. V., (1966). Properties of linear elastomeric polyurethanes. *Journal of Applied Polymer Science, 10,* 1837-1844.

Gao, Z. Z., Peng, J., Zhong, T. H., Sun, J., Wang, X. B., & Yue, C., (2012). Biocompatible elastomer of waterborne polyurethane based on castor oil and polyethylene glycol with cellulose nanocrystals. *Carbohydrate Polymers, 87,* 2068-2075.

Habibi, Y., & Dufresne, A., (2008). Highly filled bionanocomposites from functionalized polysaccharide nanocrystals. *Biomacromolecules, 9,* 1974-1980.

Habibi, Y., Goffin, A. L., Schiltz, N., Duquesne, E., Dubois, P., & Dufresne, A., (2008). Bionanocomposites based on poly(ε-caprolactone)-grafted cellulose nanocrystals by ring-opening polymerizatio. *Journal of Materials Chemistry, 18,* 5002-5010.

Lee, S. J., & Kim, B. K., (2012). Covalent incorporation of starch derivative into waterborne polyurethane for biodegradability. *Carbohydrate Polymers, 87,* 1803-1809.

Lee, S. K., Yoon, S. H., Chung, I., Hartwig, A., & Kim, B. K., (2011). Waterborne polyurethane nanocomposites having shape memory effects. *Journal of Polymer Science Part A: Polymer Chemistry, 49,* 634-641.

Liu, H., Song, J., Shang, S. B., Song, Z. Q., & Wang, D., (2012). Cellulose nanocrystal/silver nanoparticle composites as bifunctional nanofillers within waterborne polyurethane. *ACS Applied Materials & Interfaces, 4,* 2413-2419.

Ma, X. Y., & Zhang, W. D., (2009). Effects of flower-like ZnO nanowhiskers on the mechanical, thermal and antibacterial properties of waterborne polyurethane. *Polymer Degradation and Stability, 94,* 1103-1109.

Naghash, H. J., & Abili, B., (2010). Synthesis of a silicone containing allylic monomer and its uses in the waterborne polyurethane/vinyl acetate–acrylic hybrid emulsion copolymers. *Progress in Organic Coatings, 69,* 486-494.

Nikjea, M. M. A., & Tehrania, Z. M., (2010). Synthesis and characterization of waterborne polyurethane-chitosan nanocomposites. *Polymer-Plastics Technology and Engineering, 49,* 812-817.

Noble, K. L., (1997). Waterborne polyurethanes. *Progress in Organic Coatings. 32,* 131-136.

Rahman, M. M., Kim, H. D., & Lee, W. K., (2008). Preparation and characterization of waterborne polyurethane/clay nanocomposite: Effect on water vapor permeability. *Journal of Applied Polymer Science, 110,* 3697-3705.

Song, C. M., Yuan, Q. L., & Wang, D. N., (2004). Effect of the content of urea groups on the particle size in water-borne polyurethane or polyurethane/polyacrylate dispersions. *Colloid and Polymer Science, 282,* 642-645.

Wang, X., Xing, W. Y., Song, L., Yang, H. Y., Hu, Y., & Yeoh, G. H., (2012). Fabrication and characterization of graphene-reinforced waterborne polyurethane nanocomposite coatings by the sol-gel method. *Surface and Coatings Technology, 206,* 4778-4784.

Wang, Y. X., Tian, H. F., & Zhang, L. N., (2010). Role of starch nanocrystals and cellulose whiskers in synergistic reinforcement of waterborne polyurethane. *Carbohydrate Polymers, 80,* 665-671.

Xu, X., Shang, S. B., Song, Z. Q., Cui, S. Q., Wang, H. X., & Wang, D., (2011). Preparation and characterization of rosin-based waterborne polyurethane from maleopimaric acid polyester polyol. *BioResources, 6,* 2460-2470.

Xu, X., Song, Z. Q., Shang, S.B., Cui, S. Q., & Rao, X. P., (2011). Synthesis and properties of novel rosin-based water-borne polyurethane. *Polymer International, 60,* 1521-1526.

Zou, J. W., Zhang, F., Huang, J., Chang, P. R., Su, Z. M., & Yu, J. H., (2011). Effects of starch nanocrystals on structure and properties of waterborne polyurethane-based composites. *Carbohydrate Polymers, 85,* 824-831.

Figure Captions

Fig. 1. AFM image of CNs

Fig. 2. Surface morphologies of RWPU films with different content of CNs, 0 wt% (a), 10 wt% (b), and 20 wt% (c).

Fig. 3. FT-IR spectra of RWPU (a), RWPU/CNs5% (b), RWPU/CNs10% (c), RWPU/CNs15% (d), and RWPU/CNs 20%(e).

Fig. 4. TGA thermograms of RWPU (a), RWPU/CNs10% (b), and RWPU/CNs20% (c).

Fig. 5. DSC thermograms of RWPU and RWPU/CNs nanocomposites with different CNs loading: RWPU (a), RWPU/CNs5% (b), RWPU/CNs10% (c), RWPU/CN15% (d), and RWPU/CNs20% (e).

Fig. 6. Tensile strength and elongation at break of WPU (a) and RWPU (b) film incorporating with varying amount of CNs.

Tables

Table 1. Data showing of RWPU-based films: Glass transition temperature (T_g), Heat Capacity Change (ΔC_p),

Sample	T_g (°C)	ΔC_p (J g-1 K-1)
RWPU	22.54	0.64
RWPU/CNs5 %	17.13	0.64
RWPU/CNs10 %	16.95	0.60
RWPU/CNs15 %	17.07	0.74
RWPU/CNs20 %	20.80	0.63

Table 2. Data showing of WPU and RWPU composites films: Tensile Strength (σ_B), Elongation at Break (ε), and Young's modulus (E)

sample	σ_B (MPa)	ε (%)	E (MPa)
WPU	12.0	971	27.0
WPU/CNs5%	16.0	429	136.1
WPU/CNs10%	19.4	253	246.2
WPU/CNs15%	23.4	144	336.9
WPU/CNs20%	29.1	99	457.4
RWPU	28.2	267	316.2
RWPU/CNs5%	35.0	167	509.3
RWPU/CNs10%	38.8	83	699.3
RWPU/CNs15%	46.0	45	814.8
RWPU/CNs20%	52.3	22	1045.4

Images

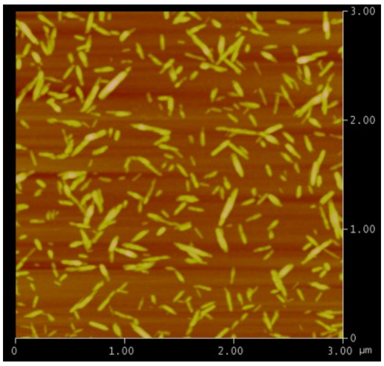

Fig. 1. AFM image of CNs

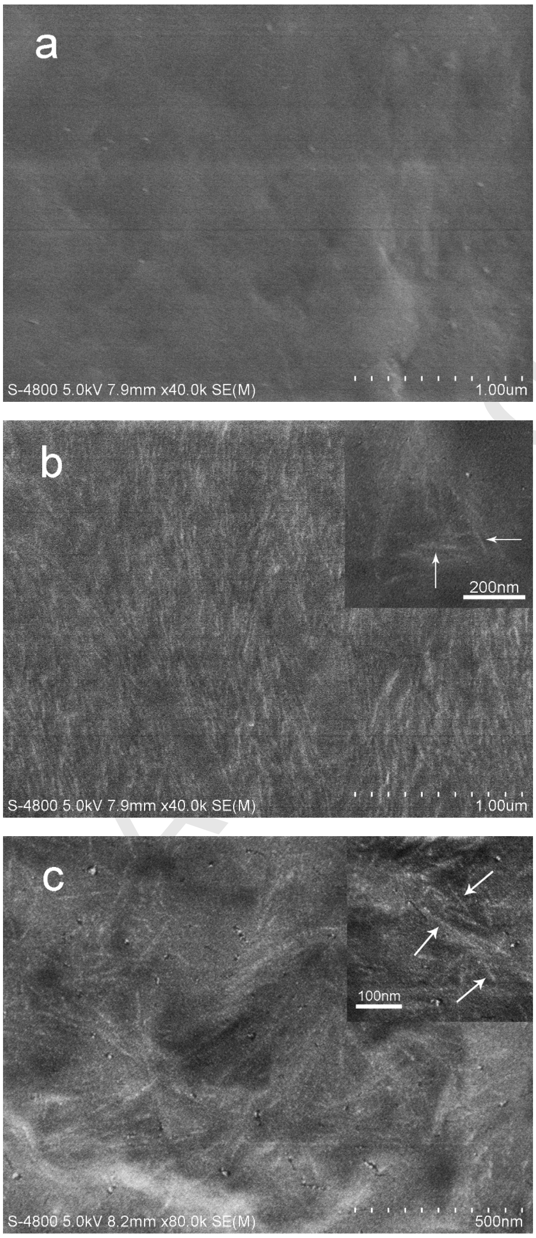

Fig. 2. Surface morphologies of RWPU films with different content of CNs, 0 wt% (a), 10 wt% (b), and 20 wt% (c).

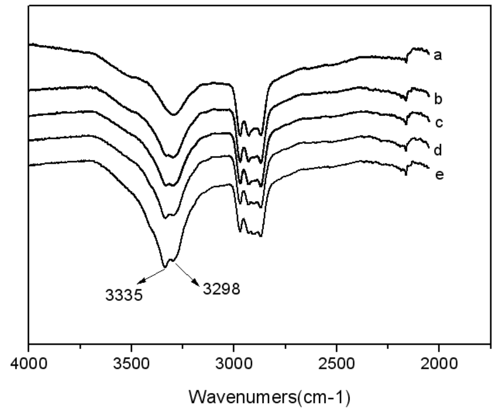

Fig. 3. FT-IR spectra of RWPU (a), RWPU/CNs5% (b), RWPU/CNs10% (c), RWPU/CNs15% (d), and RWPU/CNs 20%(e).

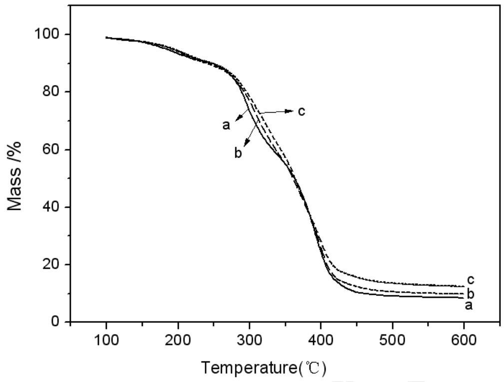

Fig. 4. TGA thermograms of RWPU (a), RWPU/CNs10% (b), and RWPU/CNs20% (c).

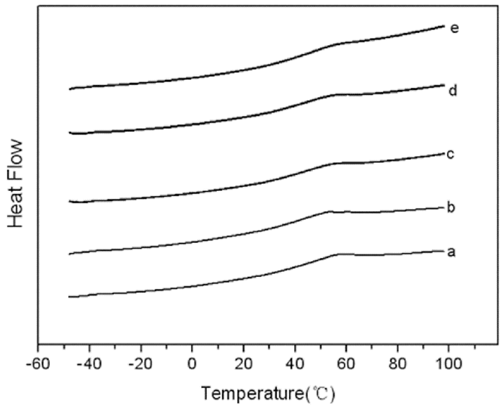

Fig. 5. DSC thermograms of RWPU and RWPU/CNs nanocomposites with different CNs loading: RWPU (a), RWPU/CNs5% (b), RWPU/CNs10% (c), RWPU/CN15% (d), and RWPU/CNs20%

(e).

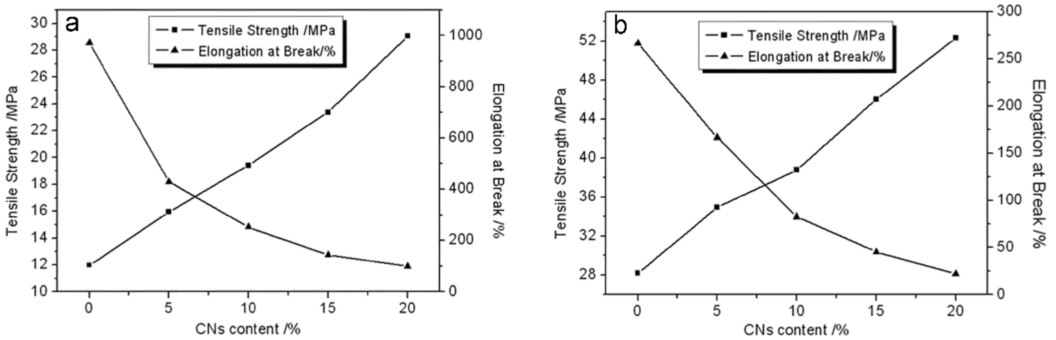

Fig. 6. Tensile strength and elongation at break of WPU (a) and RWPU (b) film incorporating with varying amount of CNs.